

Spinor boson droplets stabilized by spin fluctuations

T. A. Yoğurt ^{1,*}, A. Keleş ¹ and M. Ö. Oktel ²

¹*Department of Physics, Middle East Technical University, Ankara 06800, Turkey*

²*Department of Physics, Bilkent University, Ankara 06800, Turkey*

 (Received 24 January 2022; accepted 24 March 2022; published 13 April 2022)

Self-trapped droplets stabilized by quantum fluctuations have been experimentally realized in dipolar gases and binary boson mixtures. In this paper, we propose spinor Bose gases as another candidate for droplet formation. For spin-1 gas, we find that spin fluctuations give a dilute but self-trapped state for two different order parameters where the mean-field picture predicts collapse. A polar droplet phase can be stabilized by spin fluctuations for both antiferromagnetic and ferromagnetic spin-dependent coupling. An antiferromagnetic droplet phase can be stabilized similarly with a negative quadratic Zeeman shift. Furthermore, the beyond mean-field energy of the system depends on the quadratic Zeeman coupling, which provides a mechanism to tune the droplet formation and its density. We discuss the parameters necessary for the experimental realization of such spinor droplets.

DOI: [10.1103/PhysRevA.105.043309](https://doi.org/10.1103/PhysRevA.105.043309)

I. INTRODUCTION

Bose-Einstein condensates (BECs) have generally been modeled by the Gross-Pitaevskii (GP) mean-field (MF) approach to explain various experimental observations. Such MF theories of interacting BECs provide both a reasonable quantitative agreement and a qualitative understanding of complex phenomena, including collapse or expansion dynamics of the condensate, collective modes, bright and dark solitons, and shift of critical temperature due to interactions [1–7]. The Bogoliubov theory of weakly interacting Bose gas includes additional beyond MF processes, such as the scattering of two atoms in the condensate to states with momenta \mathbf{p} and $-\mathbf{p}$. The calculated corrections to the energy dispersion and the noncondensate depletion due to these quantum fluctuations are experimentally verified through the measurement of condensate excitations [8,9], which expose deviations from the MF theory. However, a more striking manifestation of the quantum fluctuations is the recently obtained by self-bound Bose droplets [10–12].

The traditional repulsively interacting BECs are mechanically stabilized and prevented from expansion with confining potentials based on magnetic or optical traps [1]. For attractive interactions, higher densities are energetically favorable, and the collapse of the gas to a high-density nontrapped phase can only be prevented in a metastable state, such as a bright soliton [13]. The central point of novelty in the self-bound droplets is the use of the quantum fluctuations to establish mechanically stable BECs in a regime where the MF theories predict collapse. This stability can be achieved without violating the diluteness assumption for the gas, only if separate physical parameters control the MF interaction energy and the quantum fluctuation contribution [10].

Recent experiments have realized two classes of ultracold droplets: Binary mixture droplets [11,14,15] and dipolar droplets [12,16], both of which exhibit a tunable competition among distinct interactions and relatively weak Lee-Huang-Yang (LHY) corrections that can stabilize the residual MF energy. In dipolar droplets, the long-range and short-range interactions compete at the MF level, whereas in the binary mixture droplets, the interspecies and intraspecies short-range interactions combine to form two independent parameters, which individually control the MF and quantum fluctuation corrections. In the latter, if the s -wave scattering lengths for intraspecies interactions are $a_{11} > 0$, $a_{22} > 0$, and the interspecies scattering length is $a_{12} < 0$, the residual MF interaction is proportional to $n^2 \delta a$, where $\delta a = -|a_{12}| + \sqrt{a_{11}a_{22}}$. For negative δa , the MF energy favors higher densities and drive the system to collapse. The LHY interaction energy is of the form $(a_+ n)^{5/2}$, where $a_+ > 0$ is the effective scattering length for quantum fluctuations [10]. The LHY term increases faster with density and prevents collapse. If the equilibrium density does not violate the diluteness assumption of the Bogoliubov theory, an ultradilute, yet liquidlike self-bound droplet emerges.

The experimental results of the binary mixture droplets in homonuclear [11,14] and heteronuclear [15] systems are in fair agreement with theories based on GP approximation with local LHY corrections. However, a deeper understanding of such fluctuation stabilized states is desirable for two reasons. First, better quantitative agreement with experiments is required [11,17]. Second, these systems can be used to test the validity of various theoretical proposals in quantum many-body physics. As an example, consider the unstable soft Bogoliubov modes in the theory of the binary mixture droplets [17,18]. Whereas some recent work claim that these modes can be stabilized due to exotic many-body effects, such as bosonic pairing [17] or beyond LHY contributions [19,20], other theories neglect them, claiming that the instability would

*ayogurt@metu.edu.tr

be too slow to be observed in the experiment. Broadening the family of droplets [21–26] by adding a new stabilization mechanism may lead to novel phenomena and further enhance droplet theories.

In this paper, we consider spin-1 BEC gas as a candidate for self-bound droplet formation. We show that spin fluctuations can stabilize the polar and the antiferromagnetic (AF) phases of the spin-1 gas in the parameter regime for which the MF theory predicts collapse. Spinor gas s -wave scattering lengths cannot be changed using the standard Feshbach resonances, and the currently obtained spinor gases in Na and Rb are stable against density collapse within MF theory [27–29]. However, there are proposals, such as optical Feshbach resonances [30,31], which may provide new ways to tune the gas into the droplet regime in future experiments. As more and more atom species are cooled to ultracold temperatures, it is essential to investigate the hyperfine manifolds with unstable MF ground states (GSs) and analyze the possibility of stable self-bound droplets. Whether obtained by controlling scattering lengths or through naturally occurring scattering lengths, a droplet stabilized with spin fluctuations offers additional tools to investigate the nature of the beyond-MF equilibrium, such as the quadratic Zeeman shift.

This paper is organized as follows. In Sec. II, we summarize the Bogoliubov theory of spin-1 gas and discuss possible MF magnetic orders and the stability when LHY corrections are introduced. In Sec. III, we develop the formulation of the spinor droplet within the polar spin-1 phase and present our numerical results. In Sec. IV, we derive the parallel formulation for the AF droplet phase. In Sec. V, we discuss the experimental feasibility of spinor droplet formation and present our conclusions.

II. SPIN-1 GASES: BOGOLIUBOV THEORY

We consider a BEC of spin-1 atoms with s -wave interactions under an applied uniform and static magnetic field along the z axis. We assume a low dipolar relaxation rate, which conserves the overall magnetization along the z axis. We set this conserved magnetization to zero and drop the linear Zeeman terms from the Hamiltonian. Quadratic Zeeman energy q is taken into account as in Refs. [32,33]. The Hamiltonian is given by

$$\begin{aligned} \hat{H} = & \int d\mathbf{x} \hat{\Psi}_m^\dagger(\mathbf{x}) \left(-\frac{\hbar^2 \nabla^2}{2M} + qm^2 \right) \hat{\Psi}_m(\mathbf{x}) \\ & + \frac{c_0}{2} \int d\mathbf{x} \hat{\Psi}_m^\dagger(\mathbf{x}) \hat{\Psi}_m^\dagger(\mathbf{x}) \hat{\Psi}_m(\mathbf{x}) \hat{\Psi}_m(\mathbf{x}) \\ & + \frac{c_1}{2} \int d\mathbf{x} \hat{\Psi}_m^\dagger(\mathbf{x}) \hat{\Psi}_{m'}^\dagger(\mathbf{x}) \mathbf{F}_{mn} \cdot \mathbf{F}_{m'n'} \hat{\Psi}_n(\mathbf{x}) \hat{\Psi}_{n'}(\mathbf{x}), \quad (1) \end{aligned}$$

where $\hat{\Psi}_m^\dagger(\mathbf{x})$ and $\hat{\Psi}_m(\mathbf{x})$ are creation and annihilation operators of spin-1 atoms with the magnetic quantum number m , $\mathbf{F}_{mm'} = (F_{mm'}^x, F_{mm'}^y, F_{mm'}^z)$ are the set of spin-1 matrices, represented in the basis of z -axis eigenstates, and summation over $-1, 0$, and 1 is implied with repeated indices. Density and spin coupling constants, c_0 and c_1 , are written as $c_0 = (g_0 + 2g_2)/3$ and $c_1 = (g_2 - g_0)/3$. Here, g_0 and g_2 are the bare coupling constants of the s -wave collisions of two spin-1 bosons with total spin 0 and 2, which are given in terms of the

corresponding scattering lengths $a_{0,2}$ as $g_{0,2} = 4\pi a_{0,2} \hbar^2/M$. The bare coupling constants $g_{0,2}$ are renormalized using the standard T -matrix perturbation up to the second order to remove the ultraviolet divergence in the beyond MF energy. Note that both static magnetic fields and rf pulses can be used to adjust the strength of the quadratic Zeeman energy q [34,35].

Using Bogoliubov theory, we replace the operators $\hat{a}_{\mathbf{k},m}$ with the c -numbers $\sqrt{N_0} \tau_m$ and keep the terms with $\hat{a}_{\mathbf{k} \neq 0, m}$ and $\hat{a}_{\mathbf{k} \neq 0, m}^\dagger$ up to the second order, where N_0 is the number of particles in the $\mathbf{k} = 0$ state, τ is the GS order parameter in the spin-1 manifold, and $\hat{a}_{\mathbf{k},m}$'s are the Fourier components $\hat{\Psi}_m(\mathbf{x}) = V^{-1/2} \sum_{\mathbf{k}} \hat{a}_{\mathbf{k},m} e^{i\mathbf{k}\mathbf{x}}$. Then, the effective Bogoliubov Hamiltonian for spin-1 Bose gas becomes [33]

$$\begin{aligned} \hat{H}_{\text{eff}} = & \frac{Vn^2}{2} (c_0 + c_1 \langle \mathbf{F} \rangle^2) + qN \langle F_z^2 \rangle \\ & + \sum_{\mathbf{k} \neq 0} \left\{ [\epsilon_{\mathbf{k}} - nc_1 \langle \mathbf{F} \rangle^2 + qm^2 - q \langle F_z^2 \rangle] \hat{a}_{\mathbf{k},m}^\dagger \hat{a}_{\mathbf{k},m} \right. \\ & + nc_1 \langle \mathbf{F} \rangle \cdot \mathbf{F}_{mm'} \hat{a}_{\mathbf{k},m}^\dagger \hat{a}_{\mathbf{k},m'} \\ & + \frac{nc_0}{2} (2\hat{D}_{\mathbf{k}}^\dagger \hat{D}_{\mathbf{k}} + \hat{D}_{\mathbf{k}} \hat{D}_{-\mathbf{k}} + \hat{D}_{\mathbf{k}}^\dagger \hat{D}_{-\mathbf{k}}^\dagger) \\ & \left. + \frac{nc_1}{2} (2\hat{\mathbf{F}}_{\mathbf{k}}^\dagger \hat{\mathbf{F}}_{\mathbf{k}} + \hat{\mathbf{F}}_{\mathbf{k}} \hat{\mathbf{F}}_{-\mathbf{k}} + \hat{\mathbf{F}}_{\mathbf{k}}^\dagger \hat{\mathbf{F}}_{-\mathbf{k}}^\dagger) \right\}, \quad (2) \end{aligned}$$

where $\epsilon_{\mathbf{k}} = \hbar^2 \mathbf{k}^2/2M$ is the free particle dispersion, $\langle \mathbf{F} \rangle \equiv \sum_{m,m'} \mathbf{F}_{mm'} \tau_m^* \tau_{m'}$ is the expectation value of the spin-1 order parameter, $\hat{D}_{\mathbf{k}} \equiv \sum_m \tau_m^* \hat{a}_{\mathbf{k},m}$ and $\hat{\mathbf{F}}_{\mathbf{k}} \equiv \sum_{m,m'} \mathbf{F}_{mm'} \tau_m^* \hat{a}_{\mathbf{k},m'}$ are the density and spin-fluctuation operators, respectively. The first line of (2) is the MF energy functional of the spinor BEC,

$$\frac{E_{\text{MF}}}{V} = \frac{n^2}{2} (c_0 + c_1 \langle \mathbf{F} \rangle^2) + qn \langle F_z^2 \rangle, \quad (3)$$

whereas, all the other terms within the summation constitute the quantum fluctuations. Unlike the Bose-Bose mixtures, the quantum fluctuations within the spinor gases involve not only pseudospin labeling of different components, but also true spin fluctuations.

The minimization of the spinor MF functional (3) reveals the wide variety of magnetic orders and quantum phase transitions in spin-1 systems [32], which are briefly summarized here for completeness. See Fig. 1 for a schematic phase diagram. For $c_1 < 0$ and $q < 0$, the MF ground state is ferromagnetic with order parameters $\tau^{\text{F}} = (1 \ 0 \ 0)$ or $(0 \ 0 \ 1)$ resulting in $\langle \mathbf{F} \rangle^2 = 1$ and $\langle F_z^2 \rangle = 1$. For $c_1 < 0$ and $q > 0$, the ground state depends on the strength of q : If $q > 2|c_1|n$, the order parameter becomes $\tau^{\text{P}} = (0 \ 1 \ 0)$ which is called the polar phase, and if $0 < q < 2|c_1|n$ the order parameter becomes $\tau^{\text{BA}} = (\sin \theta / \sqrt{2} \ \cos \theta \ \sin \theta / \sqrt{2})$ with $\sin \theta = \sqrt{1/2 - q/(4|c_1|n)}$, which is named as the broken-axisymmetric phase. For $c_1 > 0$ and $q > 0$, MF energy is again minimized with the polar order parameter τ^{P} . Finally, for $c_1 > 0$ and $q < 0$, the antiferromagnetic phase is obtained with order parameter $\tau^{\text{AF}} = (1 \ 0 \ 1)/\sqrt{2}$.

Let us now consider mechanical instabilities for all the MF phases. In the ferromagnetic phase one can obtain the

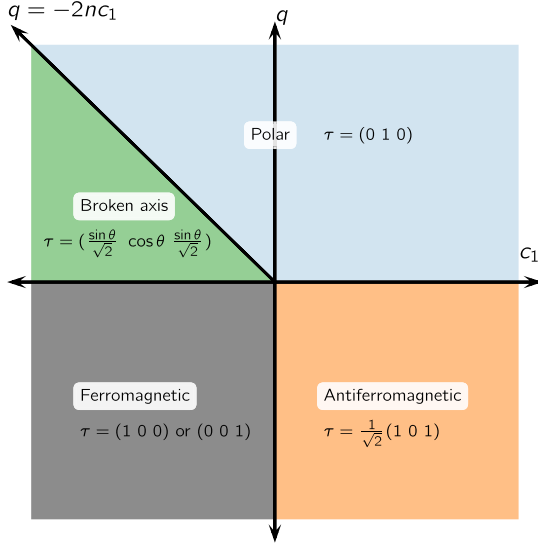


FIG. 1. Schematic phase diagram of spin-1 Bose condensate as a function of quadratic Zeeman shift q and spin-spin interaction c_1 for vanishing linear Zeeman energy $p = 0$.

MF energy density as $n^2(c_0 + c_1)/2 + qn$, which suggests a density collapse for $c_0 + c_1 \equiv g_2 < 0$. In the ferromagnetic phase, either $m = 1$ or $m = -1$ spin state exist in a uniform condensate with total conserved magnetization along z axis. This means two spin-1 bosons each having $m = 1$ (or $m = -1$) can only scatter in a single collision channel with total spin 2. Therefore, the ferromagnetic spinor gas acts as a single component BEC with the well-known LHY energy giving the following total beyond MF energy,

$$\frac{E_0^F}{V} = qn + \frac{2\pi\hbar^2 n^2}{M} a_2 \left(1 + \frac{128}{15\sqrt{\pi}} \sqrt{na_2^3} \right), \quad (4)$$

which is written in terms of scattering length a_2 for convenience. It can be seen that the collapse in the MF level with $g_2 \propto a_2 < 0$ cannot be prevented with the LHY term which comes with the same overall factor a_2 . For this reason, one cannot obtain a stability mechanism due to the LHY energy for the spinor gas in the ferromagnetic phase. We also note that LHY correction for the ferromagnetic order is independent of the quadratic Zeeman energy. A similar analysis carried out for the broken-axisymmetric phase shows that droplet formation is not possible as MF and LHY terms are controlled by the same parameter.

Consider the polar phase with $c_1 > 0$ and $q > 0$ (first quadrant in Fig. 1, which has the order parameter $\tau^P = (0 \ 1 \ 0)$) and the MF ground-state energy $E_{\text{MF}}^P = Vn^2 c_0/2$ resulting in a density collapse for $c_0 < 0$. Including the LHY corrections, the total GS energy becomes for $c_1 > 0$ and $q > 0$ [33],

$$\frac{E_0^P}{V} = \frac{n^2 c_0}{2} \left[1 + \alpha \sqrt{nc_0^3} \right] + \alpha n^2 |c_1| \sqrt{n|c_1|^3} I(t), \quad (5)$$

where $\alpha = 16\sqrt{M^3}/15\pi^2\hbar^3$, $t \equiv q/n|c_1| = |q|/n|c_1|$ since $q > 0$, and

$$I(t) \equiv -\frac{15}{8\sqrt{2}} \int_0^\infty dx x^2 \times \left(x^2 + t + 1 - \sqrt{(x^2 + t)(x^2 + t + 2)} - \frac{1}{2x^2} \right), \quad (6)$$

as shown in the Appendix, $I(t)$ can be approximated analytically as

$$I(t) \approx \frac{15\pi}{32\sqrt{2}} \left[\sqrt{t+1} - \frac{1}{32} \frac{1}{(t+1)^{3/2}} \right], \quad (7)$$

to great accuracy which will be used in the following.

Crucially, beyond MF correction in the polar phase involves contributions from density and spin fluctuations, the terms with α that are proportional to c_0 and c_1 in (5), respectively, and it also depends on the quadratic Zeeman coupling q , in stark contrast with the ferromagnetic phase discussed above. In the limit $q = 0$, $t \rightarrow 0$, and $I \rightarrow 1$, and I monotonically increases with q . Thus, spin fluctuations increase with quadratic Zeeman energy q , increasing the total GS energy. In the ultralow density limit, MF energy and density fluctuations scale with n^2 , $n^{5/2}$, respectively, whereas spin fluctuations scale with n^2 due to $\sqrt{t+1}$ term in (7). Importantly, an instability initiated in the density channel with attractive interactions at the MF level, $c_0 < 0$, can be countered with the quantum fluctuations in the spin channel c_1 , which can be controlled with the Zeeman field q whereas the fluctuations in the density channel are subleading. This observation should be compared with quantum-mechanical stabilization of Bose-Bose mixtures in Ref. [10] where a weak attractive interaction between the two components induces a MF-level instability, which is balanced by one of the two terms in the total LHY fluctuation. In contrast, the other LHY term gives a negligible “soft-mode” contributions that are routinely neglected in the literature of quantum droplets [10,14,18,36–38]. In the following, we will also ignore these fluctuations and investigate the stability condition between the MF energy in the density channel and the LHY correction in the spin channel. Our approach is similar to the work on coherently coupled two-component droplets [26,39] where the Rabi frequency plays a role similar to the Zeeman shift.

III. POLAR SPIN-1 DROPLET

For an infinite homogeneous spinor gas in the polar phase, the equilibrium between the MF and the spin-fluctuation LHY can be calculated from the condition of vanishing pressure. Using the thermodynamic identity $P = -(\partial E/\partial V)_N$, we obtain

$$P = \frac{n^2 c_0}{2} + \frac{\alpha n^2 |c_1|}{2} \sqrt{n|c_1|^3} f(t) \quad (8)$$

where $f(t) \equiv 3I(t) - 2tI'(t)$ with $f(0) = 3$. Setting this expression to zero gives the condition for the equilibrium density n_0 as

$$n_0 = \frac{|c_0|^2}{\alpha^2 |c_1|^5 f^2(t_0)}, \quad (9)$$

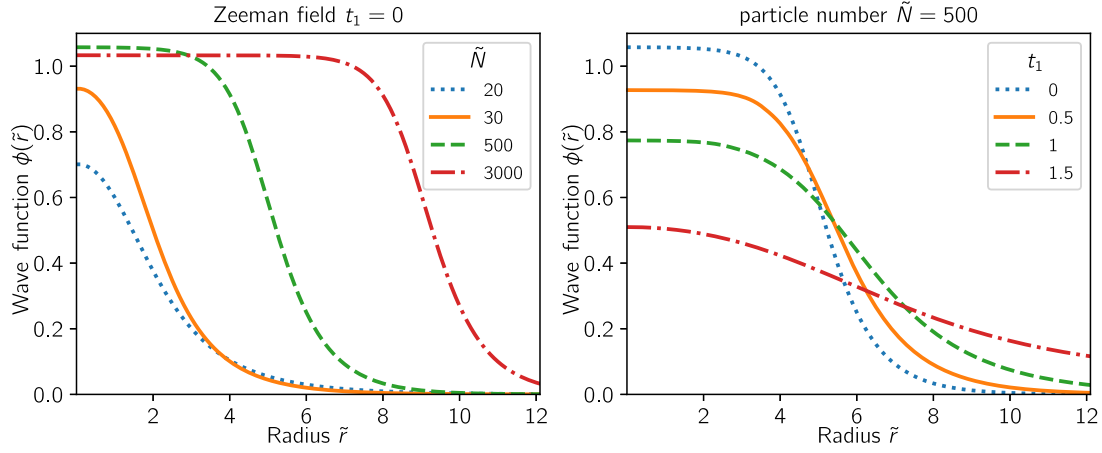


FIG. 2. The ground-state wave functions of the spin-1 gas in polar phase for various values of particle number \tilde{N} and Zeeman energy $t_1 = q/n_1|c_1|$. (Left) The wave functions for $q = 0$ (or $t_1 = 0$) and different values of \tilde{N} . Below $\tilde{N} = 20$ droplet is no longer self-trapped. (Right) The wave functions for fixed $\tilde{N} = 500$ and varying t_1 , which shows a self-bound droplet until a critical value of the quadratic Zeeman energy $q_c \approx 1.5$. The numerical calculation was performed in the radial region $\tilde{r} \in [0, 18]$.

which is an implicit equation with $t_0 = q/n_0|c_1|$. Here, n_0 also approximates the value of the saturation density in finite droplets for which the kinetic energy is negligible. Since $f(t)$ is a monotonically increasing function of t , the equilibrium density decreases with increasing quadratic Zeeman energy q . Increasing q provides a stronger LHY energy from spin fluctuations in the polar phase, and the equilibrium with the negative MF energy is reached at lower densities.

Let us study the feasibility of a finite spinor gas in the polar droplet phase more quantitatively. For a polar spinor with wave-function $\Psi(\mathbf{r}) = \psi(\mathbf{r})\tau^p$, we define the total energy functional as

$$\mathcal{E}[\psi^*, \psi] = \frac{\hbar^2}{2M} |\nabla\psi|^2 + \frac{c_0}{2} |\psi|^4 + \alpha |c_1|^{5/2} |\psi|^5 I \left[\frac{q}{|c_1| |\psi|^2} \right], \quad (10)$$

and parametrize the wave-function $\psi(\mathbf{r}) = \sqrt{n_1} \phi(\mathbf{r})$ with $n_1 = |c_0|^2 / 9\alpha^2 |c_1|^5$ obtained from (9) in the limit $q = 0$. We minimize the total energy in the grand canonical ensemble $E = \int d^3\mathbf{r} \mathcal{E}[\psi^*, \psi] - \mu N$ where the chemical potential is fixed by the total number of particles $N = \int d^3\mathbf{r} |\psi|^2$. The resulting modified GP equation is given by

$$\tilde{\mu} \phi = -\frac{1}{2} \tilde{\nabla}^2 \phi - 3|\phi|^2 \phi + \left[\frac{5}{2} I \left(\frac{t_1}{|\phi|^2} \right) |\phi|^3 - I' \left(\frac{t_1}{|\phi|^2} \right) t_1 |\phi| \right] \phi, \quad (11)$$

which is written in dimensionless form $\tilde{\mathbf{r}} = \mathbf{r}/\xi$ with $\xi = \sqrt{3\hbar^2/M|c_0|n_1}$ and $t_1 = q/n_1|c_1|$. Dimensionless chemical potential $\tilde{\mu}$ is determined from total particle number using $\tilde{N} = \int d^3\tilde{\mathbf{r}} |\phi(\tilde{\mathbf{r}})|$ and related to the total number in the droplet as $\tilde{N} = N/n_1\xi^3$.

In the limit of vanishing Zeeman energy, $q = 0$, Eq. (11) reproduces the modified GP equation of Ref. [10]. At this point, it is helpful to examine the correspondence between the polar spinor and the binary mixture droplet more closely: The MF instability condition $c_0 < 0$ in polar spinor corresponds

to $\delta g < 0$ in binary mixture, where $\delta g = g_{12} + \sqrt{g_{11}g_{22}}$ is written in terms of inter- and intracomponent coupling constants g_{12} and $g_{11}-g_{22}$, respectively. The quantum fluctuations stabilizing this instability $n^{5/2}|c_1|^{5/2}$ in polar phase corresponds to the out-of-phase term $n^{5/2}a_{\pm}^{5/2}$ in binary mixtures. The soft modes that are neglected $n^{5/2}|c_0|^{5/2}$ in the polar phase corresponds to the in-phase term $n^{5/2}a_{-}^{5/2}$ of binary mixtures.

We numerically solve the modified GP Eq. (11) to obtain the GS wave functions for various values of the quadratic Zeeman coupling q and the total number of particles \tilde{N} using imaginary time propagation. Our results are shown in Fig. 2. The left panel in Fig. 2 shows the wave functions for various values of \tilde{N} for fixed $q = 0$. The polar spinor gas forms a self-bound quantum droplet for particle numbers above the critical value near $\tilde{N}_c \approx 19$ as in the Bose-Bose mixtures [10]. Below this critical level \tilde{N}_c , the repulsive pressure due to the kinetic energy dominates the MF attraction and causes the droplet to expand to infinity. The right panel in Fig. 2 shows the GS wave functions for various values of q or t for fixed $\tilde{N} = 500$. One can see that increasing q strengthens the LHY energy of the spin fluctuations, which, in turn, decreases the maximum density of the droplet. Above a critical value of the Zeeman energy $q_c \approx 1.5$, repulsion from the LHY energy combined with the kinetic-energy quantum pressure overwhelms the MF attraction and the droplet again expands to infinity. Then, the quadratic Zeeman coupling can be used to tune the particle density at the center of the droplet. However, a finite Zeeman energy $q \neq 0$ also increases the critical value of N_c . Since the droplet wave function is Gaussian to a good accuracy around the critical region, we study the q_c vs N_c using a Gaussian ansatz and compare with the numerical solution for different values of $t_1 = q/n_1|c_1|$. As shown in Fig. 3, N_c increases with t_1 monotonically.

Polar droplet discussion has so far considered the parameter region in which $c_1 > 0$ and $q > 0$. However, the GS also has polar order with ferromagnetic coupling $c_1 < 0$ and strong Zeeman shift $q > -2nc_1$ (blue region within the second quadrant in Fig. 1). In this regime, the LHY energy is obtained by

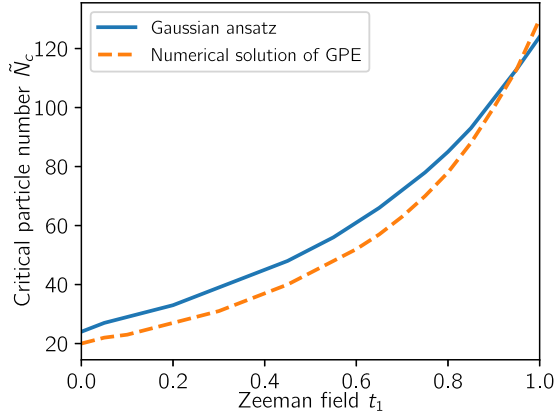


FIG. 3. The critical particle numbers \tilde{N}_c for different values of $t_1 = q/n_1|c_1|$ calculated from the numerical solution of the GP equation (orange) vs from variational calculation with the Gaussian ansatz (blue). The density at the center of the droplet decreases with q ; the kinetic energy and LHY pressure eventually overcome MF attraction.

replacing $I(t)$ with $I(t - 2)$ in all of our previous calculations. We find that droplet formation is possible for all the parameter regimes with a polar GS.

IV. ANTIFERROMAGNETIC SPIN-1 DROPLET

The AF phase realized for $c_1 > 0$ and $q < 0$ with an order parameter $\tau^{\text{AF}} = (1 \ 0 \ 1)/\sqrt{2}$ has the following total GS energy including the LHY correction:

$$\frac{E_0^{\text{AF}}}{V} = qn + \frac{n^2 c_0}{2} \left[1 + \alpha \sqrt{nc_0^3} \right] + \frac{\alpha n^2 |c_1|}{2} \sqrt{n|c_1|^3} [1 + I(t)], \quad (12)$$

where $t = |q|/nc_1 \equiv |q|/n|c_1|$ since $c_1 > 0$ here. Following the same steps given in Sec. III, we consider the collapse induced in the MF level with $c_0 < 0$ and the stabilization with the fluctuations in the spin channel and ignore the soft-mode fluctuations in the density channel. The pressure is calculated similarly as

$$P = \frac{n^2 c_0}{2} + \frac{\alpha n^2 |c_1|}{4} \sqrt{n|c_1|^3} g(t), \quad (13)$$

where $g(t) \equiv 3 + 3I(t) - 2tI'(t)$. The equilibrium density for the AF droplet is obtained from vanishing pressure as

$$n_0 = \frac{4|c_0|^2}{\alpha^2 c_1^5 g^2(t_0)}, \quad (14)$$

where $t_0 = |q|/n_0 c_1$. The equilibrium density is positive and finite since $g(t)$ is a monotonically increasing function of t for $t \geq 0$.

The total energy functional in the AF phase with wavefunction $\Psi(\mathbf{r}) = \psi(\mathbf{r})\tau^{\text{AF}}$ can be written as

$$\mathcal{E}[\psi^*, \psi] = \frac{\hbar^2}{2M} |\nabla \psi|^2 + q|\psi|^2 + \frac{c_0}{2} |\psi|^4 + \frac{\alpha}{2} |c_1|^{5/2} |\psi|^5 \left(1 + I \left[\frac{q}{|c_1| |\psi|^2} \right] \right). \quad (15)$$

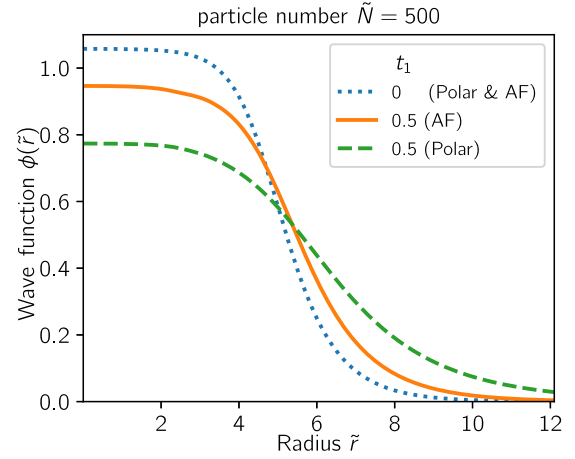


FIG. 4. Comparison of the ground-state droplet wave functions for $t_1 = -0.5, 0, 0.5$ with the particle number $\tilde{N} = 500$. The LHY energy dependence on the quadratic Zeeman shift depends on the order parameter.

We express the droplet wave function as $\psi(\mathbf{r}) = \sqrt{n_1} \phi(\mathbf{r})$ where $n_1 = |c_0|^2/9\alpha^2|c_1|^5$ is obtained from n_0 by taking the limit $q \rightarrow 0$. Defining $t_1 = |q|/n_1 c_1$ similarly, the variational minimization of energy in the grand canonical ensemble gives the following modified GP equation:

$$\tilde{\mu} \phi = -\frac{1}{2} \tilde{\nabla}^2 \phi + 3t_1 \frac{|c_1|}{|c_0|} \phi - 3|\phi|^2 \phi + \left\{ \frac{5}{4} \left[1 + I \left(\frac{t_1}{|\phi|^2} \right) \right] |\phi|^3 - \frac{1}{2} I' \left(\frac{t_1}{|\phi|^2} \right) t_1 |\phi| \right\} \phi. \quad (16)$$

This equation of motion also reduces to the same form with Eq. (11) when $q \rightarrow 0$, i.e., $t_1 \rightarrow 0$. Even though the AF phase yields the same GS wave functions with the polar case when $q = 0$, the effect of nonzero $|q|$ values are different for AF and polar cases. The AF phase stabilizes the droplet with contributions from both density and spin fluctuations, whereas the spin fluctuation is the only stabilizing mechanism in the polar case.

To investigate the stability of a finite-size AF spinor droplet, we solve the modified GP equation numerically and calculate the GS wave functions in Fig. 4. The stronger quadratic Zeeman shift again implies less density for the droplet within the central region. A further increase in $|q|$ causes the expansion of the droplet similar to the polar phase. Hence, the quadratic Zeeman effect can again be used to control the density of the droplet.

V. DISCUSSION OF EXPERIMENTAL REALIZATION AND CONCLUSION

The phase diagram and the stability of spin-1 Bose is controlled by three parameters: density-density interaction c_0 , spin-spin interaction c_1 , and quadratic Zeeman energy q . A self-trapped droplet forms when the MF instability towards mechanical collapse induced with $c_0 < 0$ is balanced with the LHY quantum fluctuations. The derivation of the LHY energy is based on a perturbative expansion within the

Bogoliubov theory and requires diluteness, which is satisfied if $|c_0|/|c_1|$ is sufficiently small. In the case of a finite droplet, additional quantum pressure coming from kinetic energy, the total particle number constraint, and the quadratic Zeeman shift give rise to a rich but complex interplay to determine the full stability.

Experimentally, the spinor BECs obtained so far are not favorable for droplet formation since they are all mechanically stable with $c_0 > 0$ [27,28,32,34,40,41]. For the most commonly used alkali-metal atoms Na and Rb, c_0 is an order of magnitude larger than $|c_1|$ [32], whereas for lithium $|c_0|/|c_1| \sim 0.46$ [42]. To our knowledge, there is no fundamental reason for c_0 to be positive or much larger than c_1 in a complicated atom-atom scattering process, and favorable parameters may emerge in a novel hyperfine manifold as more atomic gases are trapped and cooled with new species and mixtures. Furthermore, the spinor gases lack the standard magnetic Feshbach resonance for tuning the interaction strength, but there are theory proposals for scattering length tuning with optical Feshbach resonances which may soon be experimentally realized [30,31]. We want to stress that the required change for the gas to go into the self-trapped droplet regime is not extraordinarily large. Hypothetically, consider an atom with 0-channel and 2-channel scattering lengths $a_0 = -100a_B$ and $a_2 = +45a_B$, which yields $c_0 = \frac{4\pi\hbar^2}{M}(-\frac{10}{3}a_B) < 0$ and $c_1 = \frac{4\pi\hbar^2}{M}(\frac{145}{3}a_B) > 0$ with the ratio $\frac{c_0}{c_1} \simeq -0.07$. For an atom with 23-amu mass, the expected density at the center of a saturated droplet is $n_1 \approx 13 \times 10^{14} \text{ cm}^{-3}$ when $q = 0$ and a droplet with $N = 25\,000$ particles would be self-trapped. The correlation length becomes $\xi \simeq 1 \mu\text{m}$. For the total number of particles 130 000 ($\tilde{N} = 100$), the droplet will be stable up to $t_1 \simeq 1$, thus, the quadratic Zeeman shift can be varied between 0 and 20 kHz. The droplet size is in the 3–6- μm interval for $N \approx 25\,000$ to 150 000 particles.

In conclusion, similar to the droplet formations in the dipolar and binary mixture gases, we predict a self-trapped droplet

for the spin-1 gas in the polar and AF phases. The mechanism behind this stability is the competition between the MF attraction and LHY repulsion induced by spin fluctuations. The quadratic Zeeman effect can be used to control the stability of the droplet and its density. We hope that parameters favorable to droplet formation can be experimentally realized in new cold atom species or by adjusting the scattering lengths. Our results can be extended to nonzero magnetization, spin-2 gases, and spinor mixtures. Furthermore, other manifestations of the beyond MF interactions within the spinor BECs may also provide an exciting research direction.

ACKNOWLEDGMENTS

This work was supported by TUBITAK 2236 Co-funded Brain Circulation Scheme 2 (CoCirculation2) Project No. 120C066 (A.K.).

APPENDIX: ANALYTICAL APPROXIMATION FOR $I(t)$

We use a change in variable $y \equiv x^2 + t + 1$ in the integral (5) and expand $\sqrt{1 - 1/y^2}$ in Taylor series up to the second order in the domain $x \geq 0$ and $t \geq 0$ and obtain

$$I(t) = -\frac{15}{16\sqrt{2}} \int_0^\infty dx \left(\frac{-(t+1)}{x^2+t+1} + \frac{x^2}{4(x^2+t+1)^3} \right).$$

Each term above can be calculated to give

$$I(t) \approx \frac{15\pi}{32\sqrt{2}} \left[\sqrt{t+1} - \frac{1}{32} \frac{1}{(t+1)^{3/2}} \right]. \quad (\text{A1})$$

Higher-order terms in the expansion of $\sqrt{1 - 1/y^2}$ can improve the accuracy, but we numerically checked that the second-order expansion is sufficient up to less than 1% error for all t values.

-
- [1] L. Pitaevskii and S. Stringari, *Bose-Einstein Condensation and Superfluidity* (Oxford University Press, Oxford, 2016), Vol. 164.
- [2] C. J. Pethick and H. Smith, *Bose-Einstein Condensation in Dilute Gases* (Cambridge University Press, Cambridge, UK, 2008).
- [3] M.-O. Mewes, M. R. Andrews, N. J. van Druten, D. M. Kurn, D. S. Durfee, C. G. Townsend, and W. Ketterle, Collective Excitations of a Bose-Einstein Condensate in a Magnetic Trap, *Phys. Rev. Lett.* **77**, 988 (1996).
- [4] F. Dalfovo, S. Giorgini, L. P. Pitaevskii, and S. Stringari, Theory of Bose-Einstein condensation in trapped gases, *Rev. Mod. Phys.* **71**, 463 (1999).
- [5] F. Gerbier, J. H. Thywissen, S. Richard, M. Hugbart, P. Bouyer, and A. Aspect, Experimental study of the thermodynamics of an interacting trapped Bose-Einstein condensed gas, *Phys. Rev. A* **70**, 013607 (2004).
- [6] C. Mordini, D. Trypogeorgos, A. Farolfi, L. Wolswijk, S. Stringari, G. Lamporesi, and G. Ferrari, Measurement of the Canonical Equation of State of a Weakly Interacting 3D Bose Gas, *Phys. Rev. Lett.* **125**, 150404 (2020).
- [7] R. P. Smith, R. L. D. Campbell, N. Tammuz, and Z. Hadzibabic, Effects of Interactions on the Critical Temperature of a Trapped Bose Gas, *Phys. Rev. Lett.* **106**, 250403 (2011).
- [8] S. B. Papp, J. M. Pino, R. J. Wild, S. Ronen, C. E. Wieman, D. S. Jin, and E. A. Cornell, Bragg Spectroscopy of a Strongly Interacting ^{85}Rb Bose-Einstein Condensate, *Phys. Rev. Lett.* **101**, 135301 (2008).
- [9] N. Navon, S. Piatecki, K. Günter, B. Rem, T. C. Nguyen, F. Chevy, W. Krauth, and C. Salomon, Dynamics and Thermodynamics of the Low-Temperature Strongly Interacting Bose Gas, *Phys. Rev. Lett.* **107**, 135301 (2011).
- [10] D. S. Petrov, Quantum Mechanical Stabilization of a Collapsing Bose-Bose Mixture, *Phys. Rev. Lett.* **115**, 155302 (2015).
- [11] C. R. Cabrera, L. Tanzi, J. Sanz, B. Naylor, P. Thomas, P. Cheiney, and L. Tarruell, Quantum liquid droplets in a mixture of Bose-Einstein condensates, *Science* **359**, 301 (2018).
- [12] I. Ferrier-Barbut, H. Kadau, M. Schmitt, M. Wenzel, and T. Pfau, Observation of Quantum Droplets in a Strongly Dipolar Bose Gas, *Phys. Rev. Lett.* **116**, 215301 (2016).

- [13] S. L. Cornish, S. T. Thompson, and C. E. Wieman, Formation of Bright Matter-Wave Solitons During the Collapse of Attractive Bose-Einstein Condensates, *Phys. Rev. Lett.* **96**, 170401 (2006).
- [14] G. Semeghini, G. Ferioli, L. Masi, C. Mazzinghi, L. Wolswijk, F. Minardi, M. Modugno, G. Modugno, M. Inguscio, and M. Fattori, Self-Bound Quantum Droplets of Atomic Mixtures in Free Space, *Phys. Rev. Lett.* **120**, 235301 (2018).
- [15] K. E. Wilson, A. Guttridge, J. Segal, and S. L. Cornish, Quantum degenerate mixtures of Cs and Yb, *Phys. Rev. A* **103**, 033306 (2021).
- [16] M. Schmitt, M. Wenzel, F. Böttcher, I. Ferrier-Barbut, and T. Pfau, Self-bound droplets of a dilute magnetic quantum liquid, *Nature (London)* **539**, 259 (2016).
- [17] H. Hu and X.-J. Liu, Consistent Theory of Self-Bound Quantum Droplets with Bosonic Pairing, *Phys. Rev. Lett.* **125**, 195302 (2020).
- [18] P. Zin, M. Pylak, and M. Gajda, Revisiting a stability problem of two-component quantum droplets, *Phys. Rev. A* **103**, 013312 (2021).
- [19] Q. Gu and L. Yin, Phonon stability and sound velocity of quantum droplets in a boson mixture, *Phys. Rev. B* **102**, 220503(R) (2020).
- [20] M. Ota and G. Astrakharchik, Beyond Lee-Huang-Yang description of self-bound Bose mixtures, *SciPost Phys.* **9**, 20 (2020).
- [21] P. Naidon and D. S. Petrov, Mixed Bubbles in Bose-Bose Mixtures, *Phys. Rev. Lett.* **126**, 115301 (2021).
- [22] J. Sánchez-Baena, J. Boronat, and F. Mazzanti, Supersolid striped droplets in a raman spin-orbit-coupled system, *Phys. Rev. A* **102**, 053308 (2020).
- [23] Y. Ma, C. Peng, and X. Cui, Borromean Droplet in Three-Component Ultracold Bose Gases, *Phys. Rev. Lett.* **127**, 043002 (2021).
- [24] J. C. Smith, D. Baillie, and P. B. Blakie, Quantum Droplet States of a Binary Magnetic Gas, *Phys. Rev. Lett.* **126**, 025302 (2021).
- [25] R. N. Bisset, L. A. Peña Ardila, and L. Santos, Quantum Droplets of Dipolar Mixtures, *Phys. Rev. Lett.* **126**, 025301 (2021).
- [26] A. Cappellaro, T. Macrì, G. F. Bertacco, and L. Salasnich, Equation of state and self-bound droplet in rabi-coupled bose mixtures, *Sci. Rep.* **7**, 13358 (2017).
- [27] J. Stenger, S. Inouye, D. M. Stamper-Kurn, H.-J. Miesner, A. P. Chikkatur, and W. Ketterle, Spin domains in ground-state Bose-Einstein condensates, *Nature (London)* **396**, 345 (1998).
- [28] M.-S. Chang, C. D. Hamley, M. D. Barrett, J. A. Sauer, K. M. Fortier, W. Zhang, L. You, and M. S. Chapman, Observation of Spinor Dynamics in Optically Trapped ^{87}Rb Bose-Einstein Condensates, *Phys. Rev. Lett.* **92**, 140403 (2004).
- [29] H. Schmaljohann, M. Erhard, J. Kronjäger, M. Kottke, S. van Staa, L. Cacciapuoti, J. J. Arlt, K. Bongs, and K. Sengstock, Dynamics of $F = 2$ Spinor Bose-Einstein Condensates, *Phys. Rev. Lett.* **92**, 040402 (2004).
- [30] T. L. Nicholson, S. Blatt, B. J. Bloom, J. R. Williams, J. W. Thomsen, J. Ye, and P. S. Julienne, Optical feshbach resonances: Field-dressed theory and comparison with experiments, *Phys. Rev. A* **92**, 022709 (2015).
- [31] O. Thomas, C. Lippe, T. Eichert, and H. Ott, Experimental realization of a Rydberg optical Feshbach resonance in a quantum many-body system, *Nat. Commun.* **9**, 2238 (2018).
- [32] D. M. Stamper-Kurn and M. Ueda, Spinor Bose gases: Symmetries, magnetism, and quantum dynamics, *Rev. Mod. Phys.* **85**, 1191 (2013).
- [33] S. Uchino, M. Kobayashi, and M. Ueda, Bogoliubov theory and Lee-Huang-Yang corrections in spin-1 and spin-2 Bose-Einstein condensates in the presence of the quadratic Zeeman effect, *Phys. Rev. A* **81**, 063632 (2010).
- [34] T. Kuwamoto, K. Araki, T. Eno, and T. Hirano, Magnetic field dependence of the dynamics of ^{87}Rb spin-2 Bose-Einstein condensates, *Phys. Rev. A* **69**, 063604 (2004).
- [35] A. T. Black, E. Gomez, L. D. Turner, S. Jung, and P. D. Lett, Spinor Dynamics in an Antiferromagnetic Spin-1 Condensate, *Phys. Rev. Lett.* **99**, 070403 (2007).
- [36] E. Aybar and M. Ö. Oktel, Temperature-dependent density profiles of dipolar droplets, *Phys. Rev. A* **99**, 013620 (2019).
- [37] Y. V. Kartashov, G. E. Astrakharchik, B. A. Malomed, and L. Torner, Frontiers in multidimensional self-trapping of nonlinear fields and matter, *Nat. Rev. Phys.* **1**, 185 (2019).
- [38] F. Böttcher, J.-N. Schmidt, J. Hertkorn, K. S. H. Ng, S. D. Graham, M. Guo, T. Langen, and T. Pfau, New states of matter with fine-tuned interactions: Quantum droplets and dipolar supersolids, *Rep. Prog. Phys.* **84**, 012403 (2020).
- [39] L. Lavoine, A. Hammond, A. Recati, D. S. Petrov, and T. Bourdel, Beyond-Mean-Field Effects in Rabi-Coupled Two-Component Bose-Einstein Condensate, *Phys. Rev. Lett.* **127**, 203402 (2021).
- [40] J. Mur-Petit, M. Guilleumas, A. Polls, A. Sanpera, M. Lewenstein, K. Bongs, and K. Sengstock, Dynamics of $F = 1$ ^{87}Rb condensates at finite temperatures, *Phys. Rev. A* **73**, 013629 (2006).
- [41] J. Guzman, G.-B. Jo, A. N. Wenz, K. W. Murch, C. K. Thomas, and D. M. Stamper-Kurn, Long-time-scale dynamics of spin textures in a degenerate $F = 1$ ^{87}Rb spinor Bose gas, *Phys. Rev. A* **84**, 063625 (2011).
- [42] S. J. Huh, K. Kim, K. Kwon, and J.-y. Choi, Observation of a strongly ferromagnetic spinor Bose-Einstein condensate, *Phys. Rev. Research* **2**, 033471 (2020).